Vol. 554: 35–50, 2016
doi: 10.3354/meps11780

MARINE ECOLOGY PROGRESS SERIES
Mar Ecol Prog Ser

Published July 28

Benthic primary production and mineralization in a High Arctic fjord: *in situ* assessments by aquatic eddy covariance

Karl M. Attard[1,2,6,*], Kasper Hancke[1,2,3], Mikael K. Sejr[4], Ronnie N. Glud[1,2,4,5]

[1]Nordic Centre for Earth Evolution (NordCEE), University of Southern Denmark, 5230 Odense M, Denmark
[2]Greenland Climate Research Centre, Greenland Institute of Natural Resources, 3900 Nuuk, Greenland
[3]Department of Bioscience, Aarhus University, 8000 Aarhus C, Denmark
[4]Arctic Research Centre, Aarhus University, 8000 Aarhus C, Denmark
[5]Scottish Association for Marine Sciences, Scottish Marine Institute, PA37 1QA Oban, UK

[6]*Present address:* Tvärminne Zoological Station, University of Helsinki, J.A. Palménin tie 260, 10900 Hanko, Finland

ABSTRACT: Coastal and shelf systems likely exert major influence on Arctic Ocean functioning, yet key ecosystem processes remain poorly quantified. We employed the aquatic eddy covariance (AEC) oxygen (O_2) flux method to estimate benthic primary production and mineralization in a High Arctic Greenland fjord. Seabed gross primary production (GPP) within the 40 m deep photic zone was highest at 10 m (29 mmol O_2 m^{-2} d^{-1}) and decreased to 5 mmol O_2 m^{-2} d^{-1} at 40 m, while nighttime community respiration (CR) ranged from 11 to 25 mmol O_2 m^{-2} d^{-1}. CR decreased to ~2.5 mmol O_2 m^{-2} d^{-1} at 80 m and remained constant with further depth. Fauna activity accounted for ~50% of the CR at depths ≤60 m but was <15% at depths ≥80 m. Benthic GPP and CR were comparable when scaled to the outer fjord area ≤40 m depth (2.7 and 3.1 t C d^{-1}), and here the seabed was twice as important as the pelagic compartment for primary production. However, when scaled to the entire outer fjord area of which 80% is >40 m, benthic GPP was 26% of the pelagic production. CR was 2-fold higher than GPP over this region (5.7 t C d^{-1}) and thus net heterotrophic. By scaling AEC-derived Arctic benthic GPP to the entire Arctic Ocean using modelled seabed light data, we estimate an annual Arctic Ocean benthic GPP of 11.5×10^7 t C yr^{-1}. On average, this value represents 26% of the Arctic Ocean annual net phytoplankton production estimates. This scarcely considered component is thus potentially important for contemporary and future Arctic ecosystem functioning.

KEY WORDS: Benthic primary production · Carbon cycling · Arctic · Aquatic eddy covariance · Benthic macrofauna

INTRODUCTION

Coastal and shelf seas represent the interface between land and the open ocean and are regions of intensified carbon cycling. The seabed is a key compartment of this system where high densities of heterotrophic microbes and fauna mediate high rates of organic matter mineralization, sustaining continued water column production through nutrient regeneration (Middelburg et al. 2005, Glud 2008, Aller 2014). Furthermore, around a third of the global shelf seabed is predicted to support benthic primary production (Gattuso et al. 2006). Benthic algae comprising both microphytobenthos and macroalgae can be the dominant source of primary production in shallow oligotrophic waters, and their presence markedly influences the biogeochemical functioning of coastal environments (Fenchel & Glud 2000, Dalsgaard 2003, Duarte et al. 2005). However, most studies focus on the pelagic activity alone and exclude a

*Corresponding author: karl.attard@biology.sdu.dk

Publisher: Inter-Research · www.int-res.com

potentially significant contribution from the benthic community (MacIntyre et al. 1996, Cahoon 1999).

More than half of the Arctic Ocean's ~15.5 × 10^6 km^2 area is located within the relatively shallow waters of its shelf seas (Jakobsson et al. 2008). While shelf systems likely exert a major influence on Arctic Ocean functioning, key ecosystem processes such as benthic primary production and mineralization remain poorly quantified within this region. Filling this knowledge gap is particularly important given the ongoing changes in the Arctic. Reductions in sea ice cover duration, extent, and thickness, increased freshwater runoff from the surrounding landmass, and changing weather patterns are expected to affect ocean productivity (Glud & Rysgaard 2007, Arrigo & van Dijken 2011, Barber et al. 2015). This could alter the partitioning of production and mineralization processes between pelagic and benthic compartments with important implications for Arctic food webs and biogeochemical functioning of coastal waters.

Areal rates of seabed primary production and mineralization are most commonly estimated from flux measurements of O_2 between the seabed and overlying water column (termed the 'benthic O_2 exchange rate', Glud 2008). Even today, the Arctic database on benthic primary production and mineralization remains limited, and most studies employ conventional measurement techniques such as closed-chamber incubations and microprofile measurements performed under controlled conditions in the laboratory on recovered sediment and algal samples (Glud et al. 2009). Closed-chamber incubations aim to quantify the activity of the benthic compartment as a whole, while microprofiles represent spot measurements capturing processes that are predominantly microbial-mediated (Rasmussen & Jorgensen 1992, Glud et al. 2003). In recent years, the aquatic eddy covariance (AEC) technique developed by Berg et al. (2003) has increasingly been applied to quantify areal rates of seabed primary production and mineralization from continuous benthic oxygen (O_2) flux measurements covering one or more days (Hume et al. 2011, Long et al. 2013, Attard et al. 2014). In contrast to sediment incubations, AEC measurements integrate large areas (10s of m^2) of the seabed under the naturally varying *in situ* conditions, and the method can also be applied to complex benthic habitats such as those dominated by coarse sediments or by large macrobenthic communities that remain largely unstudied (Berg et al. 2007, Glud et al. 2010, Rovelli et al. 2015).

The main objective of this study was to investigate the importance of the benthic compartment for carbon cycling in a typical High Arctic coastal ecosystem. We employed the AEC method to quantify benthic primary production and mineralization rates along a depth transect ranging from shallow photic habitats to deeper aphotic sites. The *in situ* AEC flux measurements were complemented with laboratory studies and seabed image analysis to investigate the importance of benthic fauna for coastal organic carbon cycling. This dataset is compared to existing benthic activity rate estimates for the area and the wider Arctic region in general, and the relative importance of benthic primary production and mineralization is discussed within an ecosystem context on both patch- (m^2) and fjord-scales (km^2). Furthermore, based on AEC-derived seabed primary production and its drivers, we discuss the importance of benthic primary production on a regional (Arctic Ocean) scale.

MATERIALS AND METHODS

Study location

The study took place between 24 July and 10 August 2014 in outer Young Sound, a ~76 km^2 region located within the larger Young Sound/Tyrolerfjord system on the northeast coast of Greenland (74° 18′ N, 20° 18′ W; Fig. 1). Young Sound represents one of the few well-studied regions within the High Arctic. The first oceanographic measurements were performed here more than 20 yr ago, and a marine monitoring program has been in place since 2003 with the aim of establishing a long-term data series of key physical, chemical, and biological oceanographic parameters (MarinBasis, www.zackenberg.dk; Rysgaard et al. 1996, Rysgaard & Glud 2007). Sea ice forms in October and reaches a maximum thickness of ~150 cm in April. Despite downwelling surface irradiances exceeding 1000 µmol quanta m^{-2} s^{-1} in spring and early summer, marine productivity remains light-limited due to the sea ice and an overlying 20–100 cm thick snow layer that together strongly reflect and attenuate the incoming solar irradiance (Glud et al. 2007). Following intense ice melt in June and July, the degraded ice pack is rapidly exported to the Greenland Sea. Ice break-up is followed by an immediate peak in primary productivity and concurrent increases in both the vertical export of organic carbon through the water column and benthic carbon mineralization rates (Rysgaard et al. 1999, Rysgaard & Sejr 2007, Thamdrup et al. 2007). The depth of the euphotic zone (1% of surface

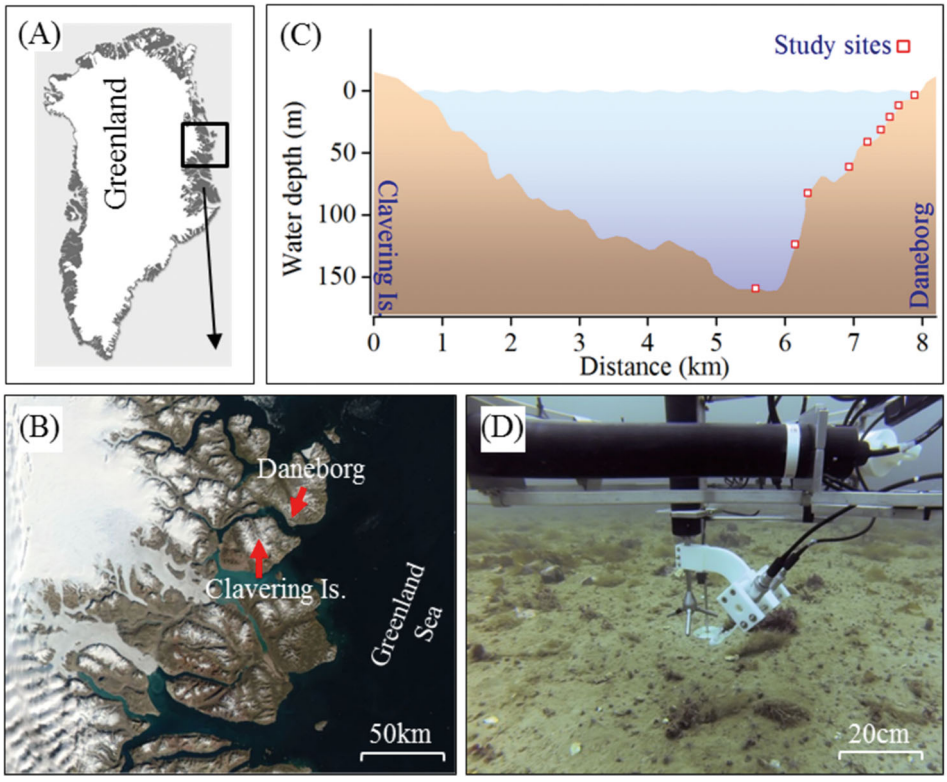

Fig. 1. (A,B) Study location near Daneborg (Young Sound) in Northeast Greenland. (B) Satellite image taken on 20 August 2014 (courtesy of the Danish Meteorological Institute). (C) Nine stations along a depth transect ranging from 5–160 m depth. (D) Image of the aquatic eddy covariance (AEC) instrumentation deployed at 20 m depth

irradiance) during the open-water period is between 25 and 40 m, although coralline algae have been observed down to 50 m (or ~0.05% surface irradiance; Roberts et al. 2002). Since 1950, the duration of the open-water period in Young Sound has ranged from 64 to 131 d (average = 88 d) with a tendency towards lengthier ice-free periods in the past 20 yr (Glud et al. 2007).

Our study considered 9 benthic stations located within a water depth transect ranging from 5 m closest to the shoreline to 160 m in the central basin of the fjord (planned depths of 5, 10, 20, 30, 40, 60, 80, 120, and 160 m). Rates of benthic metabolism were estimated from AEC measurements of O_2 fluxes. High-resolution images of the seabed were used to quantify the macrobenthic biodiversity at each station, and the microbial-mediated sediment O_2 uptake rates at the deep stations (60–160 m depth) were quantified from sediment O_2 microprofiles performed in the laboratory on sediment cores. Sediments at the deep stations consisted of cohesive muds with surface (top 10 mm) porosity ranging from 0.72 to 0.81 with an average for the 4 stations of 0.76 ± 0.03 (SD, n = 6).

Aquatic eddy covariance measurements

We used our standard AEC system setup that is similar to the original design by Berg & Huettel (2008) and has been described in detail in previous studies (McGinnis et al. 2011, Attard et al. 2015). The main hardware consisted of an acoustic velocimeter (Nortek) mounted perpendicularly onto a lightweight 130 × 90 cm stainless-steel tripod frame and 2 Clark-type O_2 microsensors that relay an amplified signal to the velocimeter via submersible amplifiers (Revsbech 1989, McGinnis et al. 2011). Each microsensor was individually tested for its quality prior to deployment and had a 90% response time of <0.5 s and a stirring sensitivity of <0.7% (Gundersen et al. 1998). Following the approach described by Holtappels et al. (2015), we estimated the flux bias due to microsensor stirring sensitivity to be <9% of the derived O_2 fluxes under the prevailing *in situ* environmental conditions. Flow velocity and O_2 microsensor output were logged in continuous sampling mode at 64 Hz. The velocimeter sampling volume was located 20–25 cm above the seabed surface with the exact distance

quantified by the instrument at the start of each deployment. Images obtained from a small camera located on the AEC frame (Fig. 1D) confirmed that the sampling height was much larger than stones and macroalgae within the vicinity of the instrument. A conductivity-temperature-depth (CTD) sensor (SBE 19 plus V2, Seabird) was installed on the frame to monitor the *in situ* environmental parameters at 2 min intervals for transmitted photosynthetically active radiation (PAR; QCP-2000, Biospherical Instruments), salinity, water temperature, depth, and O_2 concentration by means of a calibrated optode (4340, Aanderaa). The AEC system was deployed at each station for a minimum of 2 d in order to ensure that at least 1 complete 24 h time series of benthic O_2 flux measurements was available for calculation of ecosystem metabolism. The instrument was lowered to the seabed by hand from a small research vessel in areas of the seafloor that appeared relatively flat and featureless on echo-sounder recordings. The instrument's internal tilt sensors confirmed that the instrument was deployed upright and remained so throughout the deployment, with a tilt of $<\pm 4°$.

Eddy covariance data treatment

Computing high-quality AEC fluxes from the recorded 64 Hz data requires following a multiple step procedure that for the large part has been adapted from well-established terrestrial eddy covariance literature (Baldocchi 2003, Lorrai et al. 2010). In the first steps, the overall quality of the recorded data is improved by excluding low-quality data points. Points were excluded when the beam correlation was <70% and the signal-to-noise ratio was <12. The 64 Hz time series was then bin-averaged to 8 Hz. This reduces the noise in the data, and the smaller file size allows for easier data handling. Outliers in the data streams for the 3 velocity components (i.e. the horizontal [u], traverse [v], and vertical [w] components) and O_2 concentrations were removed and interpolated using the method described by Mori et al. (2007). Jumps in the O_2 concentration time series that occur due to collision of particles with the sensor were also excluded (Berg et al. 2013). The measured velocities were converted to streamline coordinates to minimize projection of horizontal fluxes into the vertical (Lorke et al. 2013). Following rotation, fluxes of O_2 were extracted from the 8 Hz dataset in units of mmol O_2 m^{-2} h^{-1} using the open-source SOHFEA software (http://sohfea.dfmcginnis.com/; McGinnis et al. 2014). The software decomposes the w and O_2 time series into mean and fluctuating components as $w(t) = \overline{w} + w'$ and $O_2(t) = \overline{O_2} + O_2'$. Fluctuating components were extracted as deviations from a least-squares linear trendline. The O_2 flux was then computed as the covariance $\overline{w'O_2'}$ (Berg et al. 2003). Implicit in this calculation is the definition of a window size that is large in comparison to the timescales of the flux-contributing turbulent eddies. Analysis of the cumulative turbulent flux co-spectra for w' and O_2' indicated that a time averaging interval of 10 min was optimal for segment analysis (McGinnis et al. 2008, Lorke et al. 2013). The last step of the processing protocol involves correction for flux loss resulting from separation distances and response time of the sensors. Here, the O_2 data are shifted in time relative to the velocity data to achieve a maximum numerical flux (McGinnis et al. 2008). The required time-shift was typically <0.5 s, which is in good agreement with the response time of the O_2 sensor (Donis et al. 2015).

Eddy covariance estimates of benthic productivity

Time series of AEC O_2 flux measurements were used to derive rates of benthic productivity for each sampled depth following standard procedures, where the continuous flux time series is separated into daytime and nighttime fluxes (Hume et al. 2011, Attard et al. 2015). The transition from day to night was identified as the point when PAR was <10% of the maximum daily irradiance value. The threshold PAR values used were 31, 13, 2.4, 0.6, and 0.5 µmol quanta m^{-2} s^{-1} at 5, 10, 20, 30, and 40 m, respectively. The average O_2 exchange rate during daytime, termed the 'net daytime O_2 production' (NDP), was then estimated as a bulk average of the fluxes when PAR ≥10% of the maximum daily value. Nighttime 'community respiration' (CR) rates were computed as the absolute value (magnitude) of average nighttime O_2 fluxes. By assuming a light-independent CR rate, benthic 'gross primary productivity' (GPP) was estimated as GPP = NDP + CR. Since CR during light typically is higher than corresponding dark rates, we regard the GPP estimates as minimum values (Glud et al. 2009).

Because the midnight sun prevented fully dark conditions from establishing at the shallow stations, we define nighttime periods within the AEC time series as the periods when seabed PAR was <10% of the maximum daily value. Seabed PAR only reached a minimum of 10 µmol m^{-2} s^{-1} at 5 m and 7 µmol m^{-2} s^{-1} at 10 m depth, and this could be sufficient to main-

tain some benthic photosynthetic activity and potentially underestimate CR. To investigate this potential issue, we computed photosynthesis-irradiance (*P-E*) relationships for the individual datasets and then extended the fitted *P-E* curve to derive the theoretical CR rate for when PAR = 0 µmol m^{-2} s^{-1}. In both cases, the theoretical 'dark' CR rate changed by <10%, which represents an insignificant bias to the data. Therefore, we consider our original CR estimates for 5 and 10 m depths as being representative of 'dark' conditions.

Rates of 'net community metabolism' (NCM, in mmol O_2 m^{-2} d^{-1}) were derived at each sampling depth to evaluate the balance between autotrophy and heterotrophy over a 24 h period. NCM was estimated directly from continuous AEC flux time series as a 24 h integration of the O_2 fluxes. When more than 24 h of flux measurements were available, as was frequently the case, the NCM was computed as a weighted average of the NDP and −CR. Weighting was performed by multiplying the hourly rates of NDP and CR by the number of daytime and nighttime hours, respectively. The NCM is then equal to $NCP_{weighted} - CR_{weighted}$. Positive NCM indicates a net release of O_2 to overlying waters over a 24 h period (net autotrophy), while negative values indicate a net heterotrophic benthic compartment.

Upscaling AEC measurements of benthic productivity

Daily rates of AEC-derived benthic GPP and CR were upscaled to the outer fjord region to estimate the importance of the benthic compartment for fjord-scale primary production and mineralization. Upscaling was performed using hypsometry data available for this region (Rysgaard et al. 2003) assuming that the AEC estimates at the 9 measurement stations were representative for their depth within the outer Young Sound region. The AEC O_2 fluxes of GPP and CR were converted to carbon equivalents assuming an O_2:DIC (dissolved inorganic carbon) of 1.0 (Glud et al. 2000, 2002).

Sediment O_2 microprofiling

Three sediment cores were collected from each of the deep stations (60, 80, 120, and 160 m) using a Kajak-sampler (KC-Denmark) fitted with 5.3 cm internal diameter core liners. The cores were transported to the laboratory where they were uncapped, fitted with a rotating magnetic stirrer, submerged in bottom water, and maintained at *in situ* temperature and air saturation. After a ~12 h relaxation period, 3 to 5 sediment O_2 concentration microprofiles with a 100 µm vertical resolution were obtained per sediment core from within areas of the sediment surface that were visibly unaffected by bioturbation. The Clark-type O_2 microsensor had a ~20 µm diameter tip and was positioned using a micromanipulator. The analog-to-digital converted sensor output was transferred to a computer where the data were stored and later calibrated against 2 known O_2 concentration points: one in the overlying oxygenated water phase and the other within the anoxic sediment (Rasmussen & Jorgensen 1992).

The O_2 porewater profiles were analyzed to determine the penetration of O_2 within surface sediments (termed the O_2 penetration depth, OPD), identified as the sediment depth with zero O_2 concentration. The O_2 concentration microprofiles were subsequently converted to depth-integrated rates of sediment diffusive O_2 uptake (DOU, in mmol O_2 m^{-2} d^{-1}) using the interpretation software PROFILE (Berg et al. 1998). This approach generated statistically sound fits (R^2 > 0.99) to the measured O_2 concentration profiles within the sediment. Input parameters for tortuosity-corrected sediment molecular diffusivity (D_s) within PROFILE was expressed as a function of porosity (φ) for the top 1.0 cm of sediment (measured; 0.76) and diffusivity in free water (D) as $D_s = D/[1 + 3(1 - \varphi)]$ (Iversen & Jorgensen 1993).

The fauna-mediated O_2 uptake rate (FOU, in mmol O_2 m^{-2} d^{-1}) was subsequently estimated as the difference between the AEC-derived CR and the DOU (FOU = CR − DOU; Rasmussen & Jorgensen 1992). The FOU indicates the collective effects of bioturbation and animal respiration on the total uptake of O_2 by the benthic compartment (Glud et al. 2003).

Quantifying macrobenthic community coverage, abundance, and respiration

Coverage and abundance of dominant seabed macrofauna and flora was estimated from high-resolution images of the seabed (Blicher et al. 2009). An underwater camera system (Ocean Imaging Systems) equipped with a strobe light and a bottom contact trigger was used to collect a minimum of 10 images from each station. Representative images for the 9 stations are shown in Fig. 2. The images each had a resolution of 3872 × 2592 pixels and covered an area of 0.31 m^2. Image analysis for coverage and abun-

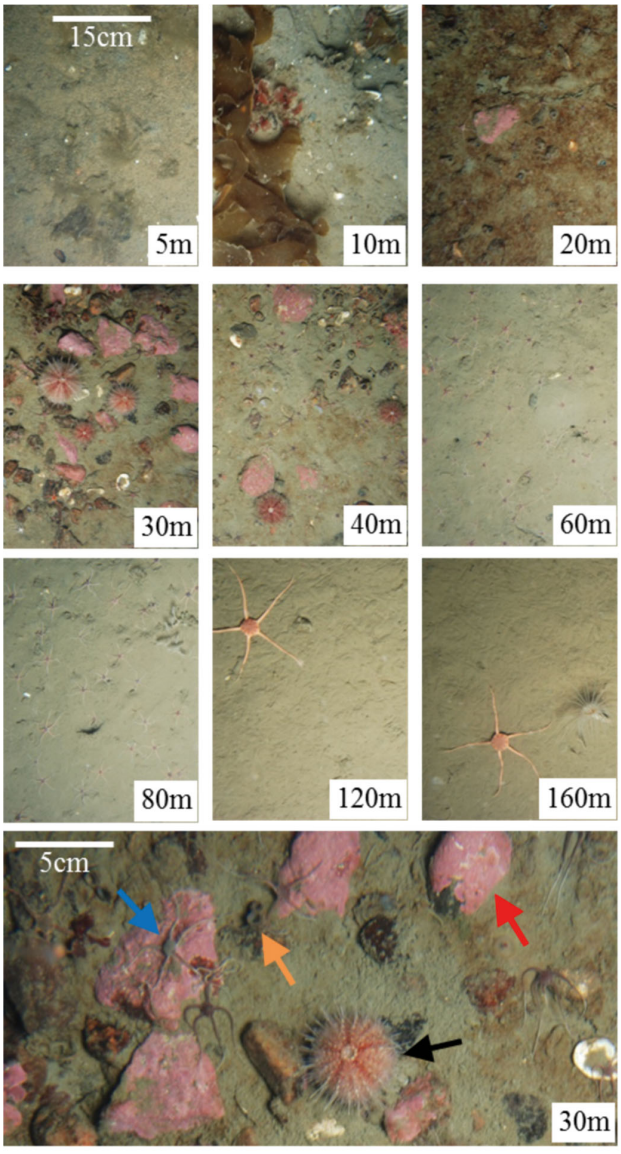

Fig. 2. Representative seabed images from the 9 measurement stations. Bottom panel is an expanded view of an image at 30 m depth showing dominant macrobenthic organisms: coralline algae (red arrow), brittle stars (*Ophiocten sericeum*, blue arrow), siphons of infaunal bivalves (*Mya truncata* and *Hiatella arctica*, orange arrow) and sea urchins (*Strongylocentrotus droebachiensis*, black arrow)

dance of the main species of flora and fauna was performed in ImageJ (http://imagej.nih.gov/ij/).

Respiration rates of dominant macrofauna groups were estimated by combining image analysis with existing empirical relationships between organism biomass or size and respiration. Respiration estimates for bivalves *Hiatella arctica* and *Mya truncata* assumed an average individual biomass based on previously reported values for Young Sound (Piepenburg et al. 1995, Sejr et al. 2004, Sejr & Christensen 2007), while the O_2 consumption by brittle stars *Ophiocten sericeum* and *Ophiopleura borealis* was estimated from the relationship between individual disc diameter and respiration rate for these species (Blicher & Sejr 2011).

RESULTS

Environmental setting

Young Sound was ice-free for the duration of the study period. Bottom waters were warmest and freshest at the shallowest stations (≤10 m depth) and became progressively cooler and more saline with depth (Table 1). Bottom waters were above saturation with respect to O_2 at depths ≤40 m (up to 108 ± 1%) and close to saturation at greater depth (down to 98 ± 1%). Daily integrated PAR measured at the seabed decreased exponentially with water depth from ~11.4 mol quanta m^{-2} d^{-1} at 5 m to ~0.2 mol quanta m^{-2} d^{-1} at 40 m depth (Table 1). Sediment (top 1 cm) chl *a* concentrations decreased with depth from 29 ± 6 mg m^{-2} at the shallowest station to 2 ± 2 mg m^{-2} at 60 m depth and remained low (~4 mg m^{-2}) down to 160 m.

Benthic fauna and flora

The sediments consisted of coarse silty sands at 5 and 10 m depth and finer silty muds and muddy silts with small glacial drop stones and gravel present at 20, 30, and 40 m (Fig. 2). Image analysis indicated that benthic faunal communities were dominated by infaunal bivalves, brittle stars, and sea urchins (Table 2). Bivalves *Mya truncata* and *Hiatella arctica* were abundant at 20, 30, and 40 m depths, up to 91 ± 40 ind. m^{-2}. Brittle stars were abundant from 20 to 80 m, with a peak abundance of 568 ± 122 ind. m^{-2} at 40 m. *Ophiocten sericeum* was the dominant brittle star at water depths <120 m whereas only the larger *Ophiopleura borealis* was observed at 120 and 160 m. The sea urchin *Strongylocentrotus droebachiensis* was observed at depths between 20 and 40 m with a peak in mean abundance of 8 ± 12 ind. m^{-2} at 40 m. Other macrobenthic organisms such as soft corals, sea lilies, and sea cucumbers were observed in lower abundances. One striking observation at the 2 shallowest stations (5 and 10 m) was the lack of conspicuous large macrofauna (Fig. 2; Table 2). These depths regularly

Table 1. Environmental conditions (±SD) during the aquatic eddy covariance (AEC) deployments at the 9 measurement stations. Data for Stns 1 to 5 are from a CTD that was mounted onto the AEC frame. For Stns 6 to 9, data for depth and water temperature were measured by the velocimeter while salinity and O_2 concentrations are values from ~1 m above the seabed extracted from CTD water column profile measurements carried out from the research vessel shortly before and after each AEC deployment. Sediment chl *a* concentrations are for top 1 cm of sediment. Number of replicate samples used to derive the average ± SD indicated in brackets. PAR: daily integrated photosynthetically active radiation (mol quanta m^{-2} d^{-1})

Stn no.	Depth (m) Planned	Actual	Water temp. (°C)	Salinity	O_2 conc. (µmol l^{-1})	O_2 conc. (% sat.)	Seabed PAR (mol m^{-2} d^{-1})	Sediment chl *a* conc. (mg m^{-2})
1	5	5.0 ± 0.4	1.3 ± 1.1	30.1 ± 1.2	384 ± 7	107 ± 2	11.43	29 ± 6 (9)
2	10	9.3 ± 0.4	0.1 ± 0.4	31.2 ± 0.3	392 ± 9	108 ± 1	5.05	13 ± 4 (13)
3	20	22.5 ± 0.4	−0.8 ± 0.3	31.7 ± 0.2	397 ± 3	107 ± 1	0.83	8 ± 5 (13)
4	30	28.8 ± 0.3	−1.2 ± 0.1	32.0 ± 0.1	393 ± 4	105 ± 2	0.23	6 ± 2 (9)
5	40	37.9 ± 0.3	−1.4 ± 0.0	32.0 ± 0.0	384 ± 3	102 ± 1	0.17	8 ± 3 (9)
6	60	62.9 ± 0.4	−1.7 ± 0.1	32.2 ± 0.0	372 ± 4	98 ± 1	–	2 ± 2 (2)
7	80	78.5 ± 0.4	−1.7 ± 0.0	32.3 ± 0.0	375 ± 1	99 ± 0	–	5 ± 2 (9)
8	120	116.2 ± 0.3	−1.7 ± 0.0	32.3 ± 0.0	375 ± 1	99 ± 0	–	4 ± 1 (9)
9	160	159.9 ± 0.3	−1.7 ± 0.0	32.3 ± 0.0	374 ± 1	99 ± 0	–	4 ± 1 (9)

Table 2. Mean (±SD) abundance and coverage of dominant groups of benthic fauna and flora (see 'Results: Benthic flora and fauna' section for species). Estimates are derived from analysis of 10 seabed images taken at each depth

Stn no.	Depth (planned, m)	Macrofauna abundance (ind. m^{-2}) Bivalves	Brittle stars	Sea urchins	Macroalgae abundance (% coverage) Filamentous	Foliose	Coralline
1	5	0	0	0	10 ± 10	5 ± 6	0
2	10	2 ± 3	1 ± 1	0	8 ± 13	21 ± 34	0
3	20	87 ± 19	75 ± 30	1 ± 2	0	0 ± 1	2 ± 2
4	30	78 ± 28	113 ± 24	6 ± 5	0	0	6 ± 4
5	40	91 ± 40	568 ± 122	8 ± 12	0	0	2 ±1
6	60	0	436 ± 96	0	0	0	0
7	80	0	278 ± 75	0	0	0	0
8	120	0	3 ± 3	0	0	0	0
9	160	0	4 ± 4	0	0	0	0

experience physical disturbances through ice grounding and scouring.

Macrofauna respiration rates were highest at 20–40 m (2.3–2.7 mmol O_2 m^{-2} d^{-1}) and decreased to 0.1–0.4 mmol O_2 m^{-2} d^{-1} at depths ≥60 m. Bivalves accounted for up to 85% of the total estimated macrofaunal respiration at depths ≤40 m. Despite high abundance of brittle stars between 20 and 80 m their combined respiration rate was in all instances <1 mmol O_2 m^{-2} d^{-1}.

Benthic flora was evident in the seabed images down to 40 m depth. Brownish mats of microphytobenthos covered most of the available sediment surface at all stations ≤40 m (Fig. 2). Soft macroalgae consisting mainly of the brown algae *Fucus* sp. and *Saccharina latissima* covered up to 21% of the seabed surface at 20 m. Coralline red algae encrusted the available rocks and stones at depths between 20 and 40 m with a maximum average seabed cover of 6% (Table 2).

AEC measurements of benthic GPP, CR, and NCM

Benthic primary productivity estimates presented herein are based on over 200 h of AEC O_2 flux measurements divided between the 5 shallow stations. The AEC fluxes were correlated with the availability of light at the seabed, where daytime O_2 fluxes were positive or less negative than nighttime values, indicating that benthic algae were actively photosynthesizing during daytime (Fig. 3, Table 3). Remarkably, this feature was also evident at 30 and 40 m depth under maximum daytime irradiances of <7 µmol quanta m^{-2} s^{-1}. Here the benthic communities exhibited high photosynthetic efficiency with very low amounts of light (1–5 µmol quanta m^{-2} s^{-1}) required to stimulate a net autotrophic response (Figs. 3 & 4). The mean flow velocity magnitude during individual deployments ranged from 0 to 12 cm s^{-1} with overall deployment averages of between 2 and 4 cm s^{-1}. Analysis of the spectra for w and O_2 indicated the

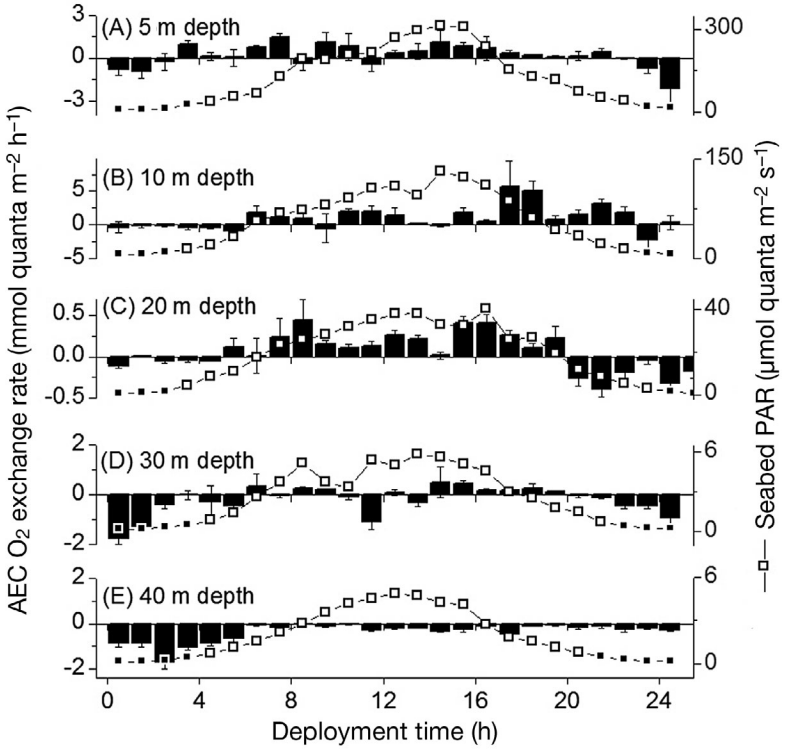

Fig. 3. (A–E) Aquatic eddy covariance (AEC) O_2 flux time series for shallow stations (5–40 m depth) overlaid with seabed photosynthetically active radiation (PAR) for a ~24 h period. (D,E) Active benthic phototrophic community evident at 30 and 40 m depth despite receiving maximum daily irradiances <7 µmol quanta m^{-2} s^{-1}. Error bars are SE (n = 6). Black squares in the PAR time series: nighttime periods

presence of an inertial subrange, and linear trends in the cumulative instantaneous flux $z'O_2'$ suggested good hydrodynamic conditions within the benthic boundary layer for AEC flux extraction. In some cases this allowed for detailed analyses to be made on controls of light on the AEC O_2 exchange rate. For instance, analysis of a high-quality 10 h section of data from 30 m depth during the transition from day to nighttime, when PAR decreased from ~7 to 0 µmol quanta m^{-2} s^{-1}, and the mean flow velocity ranged from 2 to 8 cm s^{-1} (Fig. 4A,B), suggested a clear light response in the AEC fluxes, with an apparent benthic community compensation irradiance of just ~1 µmol quanta m^{-2} s^{-1} (Fig. 4C).

The benthic community was a net source of O_2 during daytime at 5 and 10 m depth with average NDP rates of up to 0.7 mmol O_2 m^{-2} h^{-1} (Table 3), and net O_2 production exceeded consumption over a 24 h period at 5 and 10 m, with NCM rates of ~11 mmol m^{-2} d^{-1} (Table 3). The average rate of benthic GPP at 5 m of ~0.9 mmol O_2 m^{-2} h^{-1} (18 mmol O_2 m^{-2} d^{-1}) was ~1.5-fold lower than that at 10 m despite receiving more than twice as much PAR on a daily basis (Tables 1 & 3). Thereafter, benthic GPP decreased with depth in line with the availability of -transmitted PAR (Tables 1 & 3). However, while PAR decreased exponentially with water depth, the decrease in benthic GPP from 10 to 40 m depth was linear (R^2 = 0.92), presumably due to photosynthetic acclimation and variations in biomass of active phototrophs. Despite substantial primary production, the benthic communities at 20, 30, and 40 m depth were net heterotrophic.

High average nighttime CR rates up to 1.0 mmol O_2 m^{-2} h^{-1} (25 mmol O_2 m^{-2} d^{-1}) at 20 m depth indicate substantial benthic heterotrophic activity. The CR

Table 3. Mean aquatic eddy covariance (AEC) O_2 fluxes (±SE): net daytime O_2 production (NDP), nighttime community respiration (CR), gross primary production (GPP), and net community metabolism (NCM) for Stns 1 to 9 (Stns 6 to 9 were beyond the photic zone, hence no NDP or GPP). Direction of the O_2 flux is indicated by negative (uptake) and positive (release) values. AEC dataset length indicates the number of hours of AEC data used to derive the flux estimates

Stn no.	Depth (planned, m)	AEC dataset length (h)	NDP (mmol m^{-2} h^{-1})	CR (mmol m^{-2} h^{-1})	GPP (mmol m^{-2} h^{-1})	Hours of day/night	NCM (mmol m^{-2} d^{-1})
1	5	44	0.46 ± 0.11	0.46 ± 0.21	0.92 ± 0.23	20.5/3.5	11.0
2	10	33	0.65 ± 0.13	0.78 ± 0.30	1.43 ± 0.33	20.5/3.5	10.6
3	20	37	−0.18 ± 0.06	1.03 ± 0.27	0.85 ± 0.28	20.4/3.6	−7.4
4	30	44	−0.28 ± 0.07	0.73 ± 0.12	0.45 ± 0.14	15.7/8.3	−10.5
5	40	43	−0.16 ± 0.02	0.46 ± 0.06	0.30 ± 0.06	15.7/8.3	−6.3
6	60	6[a]	–	0.21 ± 0.09	–	0/24	−5.0
7	80	25	–	0.10 ± 0.01	–	0/24	−2.4
8	120	28	–	0.11 ± 0.01	–	0/24	−2.6
9	160	24	–	0.10 ± 0.01	–	0/24	−2.4

[a]Deployment cut short due to sensor damage

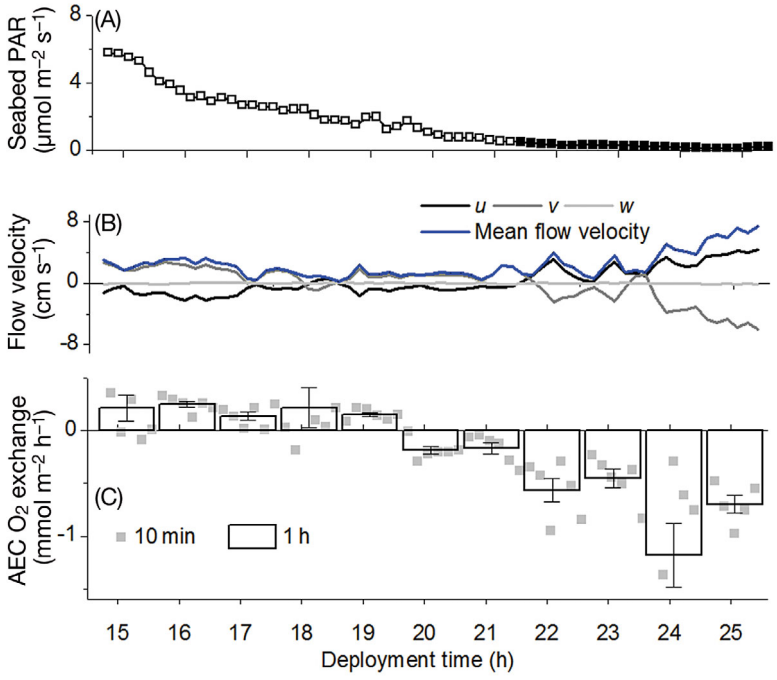

Fig. 4. (A) A 10 h time series from 30 m depth of *in situ* seabed photosynthetically active radiation (PAR). Black squares in the PAR time series: nighttime period. (B) Flow velocity within the benthic boundary layer: horizontal (u), traverse (v), and vertical (w) components. (C) Corresponding O_2 flux rates measured using aquatic eddy covariance (AEC). Little light (1–2 µmol quanta m^{-2} s^{-1}) was required to stimulate a net autotrophic response at this station. Error bars are SE (n = 6)

rates generally decreased with water depth to ~0.1 mmol O_2 m^{-2} h^{-1} at 80 m and remained relatively constant thereafter down to the deepest section of the fjord at 160 m depth (Tables 3 & 4). At these deep stations (60–160 m depth), the mean flow velocity within the benthic boundary layer as measured by the instrument ~25 cm above the sediment surface ranged from 0 to 4 cm s^{-1} with deployment averages of between 0.5 and 2.0 cm s^{-1}. Several hours of the time series were characterized by mean flow velocities <1 cm s^{-1} and suppressed exchange rates of O_2. This resulted in high temporal variability in the AEC O_2 exchange rates on short time scales (Fig. 5). While the variability in AEC O_2 fluxes in these cases likely reflects neither a variable benthic O_2 demand nor a flow-induced uptake of O_2 by the seabed, the averaged value over the entire deployment duration, which was typically ≥24 h, provides a robust measure of the benthic O_2 exchange rate (Holtappels et al. 2013). Thus, the AEC benthic O_2 uptake rate measurements for these stations are presented as a bulk average over the entire deployment duration (Tables 3 & 4).

Upscaled estimates of benthic GPP and CR for outer Young Sound

Daily AEC-derived benthic GPP and CR rates were upscaled to the area of the outer fjord ≤40 m depth to evaluate the balance between GPP and CR over the sunlit region of the seabed. Here benthic GPP and CR were comparable with daily rates of 2.7 and 3.1 t C d^{-1}, respectively. Upscaling was subsequently performed for the whole outer section of the fjord (76 km^2) including the deeper aphotic sediments that constitute around 80% of the outer Young Sound region by area. Here CR was ~2-fold higher than GPP (5.7 t C d^{-1}), indicating that the seabed was overall net heterotrophic during the summer of 2014 and required an input of organic matter from external sources to maintain the benthic carbon deficit.

Sediment DOU and FOU

Sediment O_2 microprofiles measured on cores recovered from the deeper stations (60–160 m) indicated an OPD ranging from 11.1 ± 2.2 mm (SD; n = 5) at 60 m depth to 17.8 ± 0.9 mm (SD; n = 4) at 80 m depth (Fig. 6). The average rates of benthic DOU were comparable at all depths, ranging from 2.2 to 2.8 mmol O_2 m^{-2} d^{-1}. The difference between the AEC-resolved CR rate and the DOU reflects the FOU (respiration and bioturbation). CR was ~2-fold higher than the DOU at 60 m depth (2-sample t-test p = 0.04), but the 2 methods resolved similar mean flux magnitudes for 80, 120, and 160 m that were not statistically different at the p = 0.05 level (Table 4).

DISCUSSION

Fauna contributions to benthic O_2 uptake rates

Despite low water temperature and a short productive season, large coastal regions of the Arctic sustain a high abundance and biomass of benthic macrofauna that is comparable to benthic habitats at lower latitudes (Piepenburg et al. 1995, Sejr et al. 2000, Blicher et al. 2009, Grebmeier et al. 2015). Benthic fauna contribute to the seabed O_2 consumption in 2 ways, namely directly, through respiration, and indirectly, through sediment reworking and ventilation (Kris-

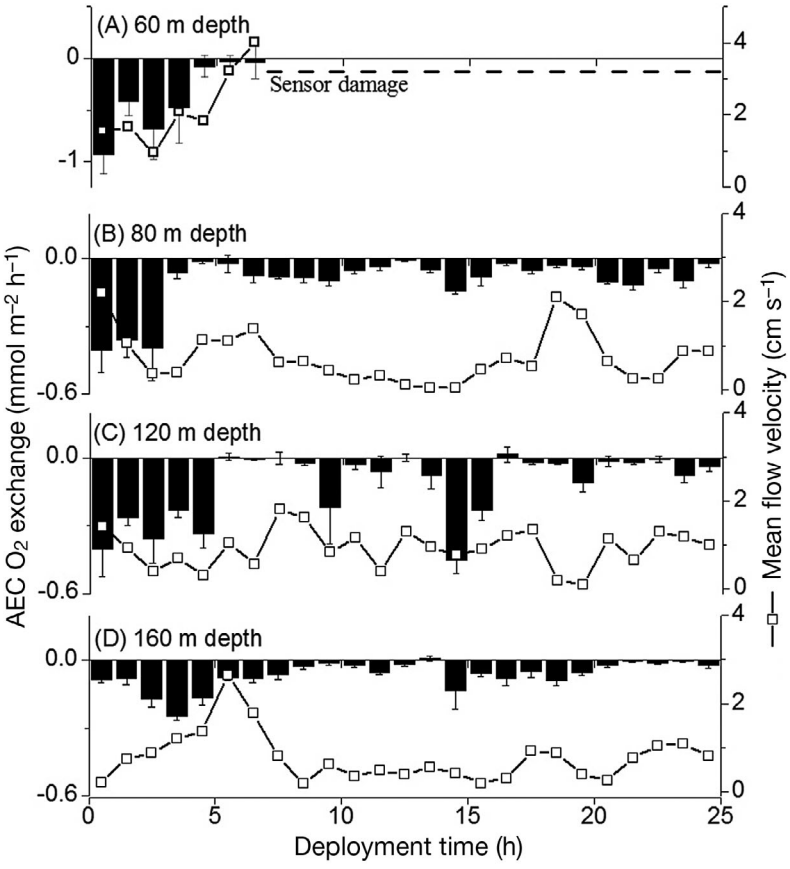

Fig. 5. Aquatic eddy covariance (AEC) O_2 flux time series for deep stations (60–160 m depth) overlaid with mean flow velocity at the seabed as measured by the instrument ~25 cm above the sediment surface. Error bars are SE (n = 6)

tensen et al. 2012). In this study, respiration rates of dominant macrofauna groups were estimated by combining image analysis with existing empirical relationships between organism biomass or size and respiration. Using this approach, respiration of dominant macrofaunal groups in Young Sound accounted for 0–24% (average = 9%) of the daily AEC-derived CR flux magnitudes for the 5–160 m depth range (Table 4, Fig. 7). Other animal groups not included in this estimate such as polychaetes are only expected to contribute minimally to total animal respiration in Young Sound, with a maximum of <0.2 mmol O_2 m^{-2} d^{-1} at 20 m depth (Glud et al. 2000, Sejr & Christensen 2007). While macrofauna respiration was a small component of the overall benthic O_2 uptake rate, bioturbation effects on the benthic O_2 consumption can be at least as important as the respiratory requirements of the animals themselves (Christensen et al. 2000, Quintana et al. 2013). Bioturbation increases the oxic volume of sediment deposits, stimulates aerobic microbial activity, and enhances the chemical oxidation of reduced products of anaerobic decay by introducing O_2 into an otherwise anoxic environment (Aller 2014). Bioturbation and animal respiration effects (collectively termed FOU) on benthic O_2 demand are most commonly quantified together as the difference between diffusive and total benthic O_2 exchange rate measurements (Rasmussen & Jorgensen 1992). Our analyses indicate that FOU could account for as much as 50% of the CR rate at 60 m water depth, which is typical for coastal settings (Glud 2008, Table 4). At greater depth, however, the DOU is seen to approximate the CR, indicating that faunal contributions are minimal. Here, macrofaunal abundance is lower, the sediment OPD larger, and the macrobenthic community is dominated entirely by deposit-feeding brittle stars *O. sericeum* and *O. borealis* whose relative contribution to benthic O_2 uptake is marginal (Blicher & Sejr 2011; Fig. 2, Table 4).

Most estimates of the FOU in coastal environments are based on the difference between incubation-derived estimates of total benthic O_2 uptake (TOU) and microprofile DOU measurements (Rasmussen & Jorgensen 1992, Glud et al. 2003). Sediment incubations typically enclose a 0.1 m^2 area of seabed or less and the incubation time is restricted to a few hours to avoid build-up of artefacts within the chamber. However, many coastal benthic habitats exhibit spatial and temporal variability in their benthic O_2 exchange rate on scales that are large in comparison to the scales included in chamber measurements, and in the absence of adequate replication this could result in a poor approximation of the true benthic activity (Glud & Blackburn 2002, Wenzhofer & Glud 2004, Berg et al. 2013). In this respect, the AEC method is particularly useful in its ability to provide non-invasive, continuous flux measurements over large spatial (10 s of m^2) and temporal (one or more days) scales from a single instrument deployment (Rheuban & Berg 2013). Following the parameterization by Berg et al. (2007), we estimated the AEC flux footprint area during this campaign to be on the order of 20–40 m^2. This would include the effects of sparsely distributed macroalgae as well as large macrofauna within the flux measurements, such as bivalves *Hiatella arctica* and *Mya truncata* that live deep (10–20 cm) within the sediment. Bivalves in

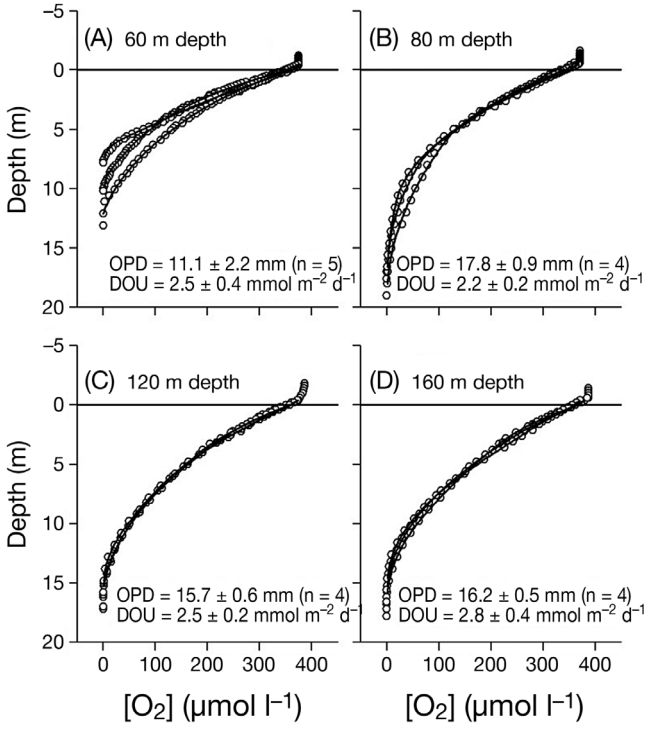

Fig. 6. Three representative sediment O_2 microprofiles for each of the deep stations (60–160 m water depth). Areal rates of sediment diffusive O_2 uptake (DOU) were computed using the O_2 concentration profile interpretation software 'PROFILE' (Berg et al. 1998) which produced fits (black lines) to the measured data (open circles). The line $y = 0$ represents the location of the sediment surface. OPD: oxygen penetration depth

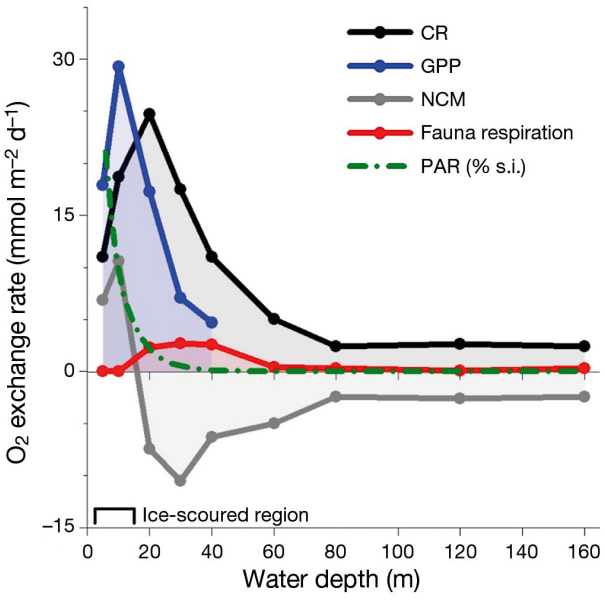

Fig. 7. Aquatic eddy covariance (AEC) measurements of daily benthic gross primary production (GPP), nighttime community respiration (CR), and net community metabolism (NCM) as a function of bathymetric depth in Young Sound. Fauna respiration was estimated from the empirical relationship between organism size or biomass and respiration. The shallowest stations (5 and 10 m depth, marked at the bottom) regularly experience disturbance through ice grounding and scouring. Water column irradiance (photosynthetically active radiation, PAR) profile is presented with units of % downwelling surface irradiance (s.i.)

Young Sound are most abundant at the 20–40 m bathymetric depth range, with average abundance ranging from 78 to 91 ind. m^{-2} (Table 3). Our CR rates for these depths are 20–40% higher (average = 30%) than existing TOU rates for the same station locations quantified using sediment core O_2 incubations (Glud et al. 2000). This difference could reflect the O_2 demand of large organisms on the seafloor that would most likely be underrepresented in core incubation measurements (Glud et al. 1998, Glud & Blackburn 2002). Interannual variations in productivity may have also contributed to these discrepancies.

Table 4. Estimates of daily total benthic O_2 demand (community respiration, CR), microbial-mediated (DOU) and fauna-mediated (FOU) O_2 uptake rates (respiration and bioturbation, FOU = CR − DOU), and respiration rates of dominant macrofauna groups alone (no DOU or FOU data available for Stns 1 to 5). *Significantly different (p = 0.04)

Stn no.	Depth (planned, m)	CR (mmol m^{-2} d^{-1})	DOU (mmol m^{-2} d^{-1})	FOU (mmol m^{-2} d^{-1})	Macrofauna respiration (mmol O_2 m^{-2} d^{-1})
1	5	11.0 ± 5.1	–	–	0
2	10	18.7 ± 7.5	–	–	0.0 ± 0.0
3	20	24.8 ± 6.5	–	–	2.3 ± 0.3
4	30	17.5 ± 2.9	–	–	2.7 ± 2.4
5	40	11.1 ± 1.4	–	–	2.6 ± 0.8
6	60	5.0 ± 1.2	2.5 ± 0.4	2.5 ± 1.3*	0.4 ± 0.0
7	80	2.4 ± 0.3	2.2 ± 0.2	0.2 ± 0.4	0.3 ± 0.0
8	120	2.6 ± 0.3	2.5 ± 0.2	0.1 ± 0.4	0.1 ± 0.0
9	160	2.4 ± 0.3	2.8 ± 0.4	−0.4 ± 0.5	0.3 ± 0.1

Benthic organic carbon cycling in Young Sound

Rates of benthic organic carbon cycling as resolved by the AEC method in Young Sound indicate high rates of organic matter synthesis and mineralization, with GPP and CR rates of up to 29 and 25 mmol O_2 m^{-2} d^{-1}, respectively (Table 3, Fig. 7). Despite year-round cold bottom

water temperatures, the benthic ecosystems are able to mediate high rates of ecosystem carbon cycling that are comparable in magnitude to many shallow-water benthic habitats at lower latitude such as those in sub-Arctic and temperate settings (Glud et al. 2010, Attard et al. 2014, 2015). This observation is in line with studies performed in other permanently cold settings, indicating that the overall community level efficiency of mineralization and benthic primary production does not depend strongly on ambient water temperature (Kostka et al. 1999, Hancke & Glud 2004, Woelfel et al. 2010).

Benthic GPP and CR showed comparable daily rates (2.7 and 3.1 t C d^{-1}, respectively) when scaled to the outer fjord area at ≤40 m depth. On average, the seabed was twice as important as the pelagic compartment for GPP in this area (~1.4 t C d^{-1}), with the latter estimate assessed from short-term ^{14}C incubations performed at several depths within the photic zone (Rysgaard et al. 1999). However, when scaled to the entire 76 km^2 outer fjord region (having 80% of its area located at depths >40 m), the estimated daily rate of benthic GPP was equivalent to 26% of the pelagic phytoplankton production. Daily benthic CR was ~2-fold higher than GPP over this same region (5.7 t C d^{-1}). Therefore, the benthic compartment was overall net heterotrophic during summer of 2014 and required an additional input of organic matter from the surrounding environment amounting to ~3.0 t C d^{-1}. The benthic C deficit was maintained through sedimentation of particulate organic matter originating from pelagic (phytoplankton, faecal pellets) and terrestrial (river discharge) sources (Rysgaard & Sejr 2007). For the large part, our AEC-derived estimates of benthic GPP and CR, and the inferences that we draw from these, are in good agreement with previous estimates of benthic primary production and mineralization for this area that are based on different methodological approaches (Krause-Jensen et al. 2007, Thamdrup et al. 2007).

Coastal benthic habitats in the Arctic are highly dynamic and typically experience high sediment and freshwater loading from river input and ice melt, current- and wave-induced sediment resuspension, grounding and scouring by drift ice, and large variations in water temperature and salinity (Hop et al. 2002, Zacher et al. 2009). The high frequency of disturbances combined with slow colonization and development means that macrobenthic communities inhabiting shallow environments are likely to be in a year-round state of recovery (Gutt 2001, Conlan & Kvitek 2005). The reduced rates of benthic GPP and CR at the shallowest stations in our study highlight the potential importance of these disturbances in influencing shallow-water biogeochemical functioning.

Light availability as a predictor of benthic primary production in the Arctic

Our daily benthic GPP estimates for depths ≤40 m are on average ~2-fold higher than the areal depth-integrated phytoplankton production rates measured using the ^{14}C-bicarbonate incubation method in Young Sound (Rysgaard et al. 1999). Indeed, seafloor primary production is frequently the dominant source of organic carbon in Arctic waters ≤40 m depth (Krause-Jensen et al. 2007, Glud et al. 2009, Woelfel et al. 2010). Because benthic primary production is measured at small scales relative to the vastness of shelf areas, scaling up the effects of local processes to larger extents is required in order to get a broad-scale perspective (Gattuso et al. 2006, Glud et al. 2009). Light is expected to be the dominant driver of benthic GPP, since nutrients usually are in steady supply following efficient mineralization of organic matter at the seabed (MacIntyre et al. 1996, Cahoon 1999). In a compilation of all available AEC-derived benthic GPP measurements for the Arctic, comprising the studies by Glud et al. (2010), Attard et al. (2014) and our present study, we found the daily benthic GPP rates to be highly correlated with the amount of daily PAR reaching the seabed (Fig. 8). It should be noted that each of the 27 data points used in this analysis is calculated from AEC O_2 flux time series which each range in duration from several hours to several days. Furthermore, while all 3 studies employ standard data processing protocols for AEC flux extraction, this comparison integrates substantial heterogeneity by considering different geographic locations, seasons, sediment types, water depths, environmental conditions, and benthic communities of algae and fauna. As a result, one could expect a substantial scatter in the data due to variations in photosynthetic biomass, ambient light acclimation and other factors that may influence production. For instance, the 2 highest benthic GPP rates of 94 and 66 mmol O_2 m^{-2} d^{-1} were measured in a sub-Arctic Greenland fjord under high daily irradiance levels in spring and early summer, respectively, in a period that coincided with substantial macroalgal growth on the seabed (Attard et al. 2014). Similarly, 7 of the 9 AEC-derived daily GPP estimates that were collected under low-light conditions (<2 mol quanta m^{-2} d^{-1}) fall above the linear regression (Fig. 8), potentially indicating a low-light acclimation of the

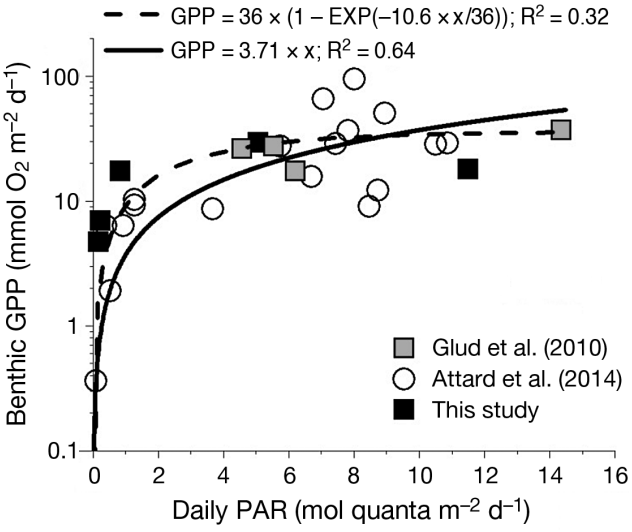

Fig. 8. Daily benthic gross primary production (GPP) rates (*y*-axis, log scale) vs. irradiance (photosynthetically active radiation, PAR): an analysis of available aquatic eddy covariance (AEC) data for the Arctic. Broken line is the exponential fit by Platt et al. (1980). The fitting parameters for the maximum rate of GPP (P_{max}) and the initial slope alpha (α) are 36 mmol O_2 m^{-2} d^{-1} and 10.6 mmol O_2 m^{-2} d^{-1} [mol quanta m^{-2} d^{-1}]$^{-1}$, respectively. The light saturation parameter ($E_k = P_{max}/\alpha$) is 3.4 mol quanta m^{-2} d^{-1}

benthic phototrophic communities (Kuhl et al. 2001, Borum et al. 2002, Attard et al. 2014). Notwithstanding these variations, the resulting relationship between the daily PAR and GPP values for the 3 studies, with a coefficient of determination (R^2 value) of 0.64, indicates that light availability alone can be used as a reasonably good predictor of benthic primary productivity in naturally heterogeneous Arctic settings. This observation provides us with an independent approach for upscaling benthic GPP measurements to the wider Arctic based on non-invasive AEC measurements and existing seafloor light availability data.

Large-scale spatial estimates of light transmittance into Arctic waters have been derived from ocean colour remote sensing data (Gattuso et al. 2006). This is an innovative and valuable approach that fills a clear knowledge gap in the sparsely sampled Arctic Ocean; however, the accuracy of the light transmittance estimates is somewhat limited due to the coarse resolution of the remote sensing data as well as the parameterization used to convert reflectance into transmitted irradiance (Gattuso et al. 2006). For instance, irradiance estimates are available at a monthly temporal resolution and include only periods when light levels were within the detection limit of the SeaWifs sensor (June to October). *In situ* measurements of benthic primary production in the Arctic document a year-round active phototrophic benthic compartment (Attard et al. 2014), indicating that benthic communities mediate primary production outside of these 5 months (albeit at a reduced daily rate). Furthermore, the spatial accuracy of the remote sensing data is limited by the grid resolution of ~25 km^2 that will exclude coastal regions such as narrow fjords and shallow embayments that are numerous in the Arctic. Naturally, these uncertainties will add on to those already described above for the benthic GPP versus light relationship and will propagate into the Arctic-wide benthic GPP estimate. At present, this is the best available approach and constitutes an important tool for obtaining a first-order estimate of the importance of benthic primary production on an Arctic Ocean scale. To do this, the light transmittance data from Gattuso et al. (2006), consisting of 240 267 grid values per month (in units of mol quanta m^{-2} d^{-1}) and covering an area of 6 126 726 km^2, were converted to daily benthic GPP using the linear relationship that we established between daily benthic GPP and seabed PAR, i.e. GPP $\times$ 3.71 $\cdot$ PAR (Fig. 8). The units (in mmol O_2 m^{-2} d^{-1}) were converted to t C km^{-2} d^{-1} assuming a photosynthetic quotient (O_2:DIC) of 1.0 (Glud et al. 2002, 2009), and the grid values were integrated to provide monthly estimates of benthic GPP for the entire Arctic Ocean. The annual Arctic benthic GPP estimate, computed as the sum of these 5 monthly values, is 11.5×10^7 t C yr^{-1}. Replacing the linear regression with the exponential function by Platt et al. (1980) improves the fit to the low-light measured daily GPP data and increases the Arctic-wide benthic GPP estimate by 15% (Fig. 8). Recent estimates of Arctic Ocean annual net phytoplankton production based on ocean colour remote sensing range from 2.0×10^8 to 9.9×10^8 t C yr^{-1} (average = 5.4×10^8 t C yr^{-1}, Babin et al. 2015). Benthic GPP is therefore equivalent to between 12 and 57% (average = 26%) of Arctic Ocean annual net phytoplankton production.

Despite the limitations of the upscaling approach presented herein, this exercise documents the importance of benthic primary production on local and regional scales in the Arctic. Our measurements document that the benthic compartment can be the dominant source of primary production in ice-free waters ≤40 m deep. Benthic primary production contributed a significant 26% of ecosystem primary production when scaled to the entire outer fjord region having 80% of its area located at depths >40 m. Based on the analysis presented above, benthic primary production also plays a substantial role in sus-

taining shelf ecosystems on an Arctic Ocean scale. Moreover, the benthic community is expected to become quantitatively more important for coastal primary production and mineralization in the future in line with expanding open-water seasons that have already increased in duration by up to 3-fold in some sectors of the Arctic since 1979 (Barnhart et al. 2014). However, even today, benthic carbon cycling remains largely under-studied and is scarcely considered in Arctic Ocean ecosystem studies. Unlike pelagic production, the benthos cannot be assessed from remote observations, and thus benthic phototrophic activity needs to be quantified in field studies on small scales. Combining *in situ* measurements of productivity with remote, large-scale observations of its drivers is likely to be an important approach for providing broad-scale estimates. In this respect, long-term measurements of primary productivity and mineralization, particularly in the vast shelf areas that experience low seabed light levels in summer, would better constrain the role of the seabed in contemporary and future Arctic Ocean functioning.

Acknowledgements. We thank Tage Dalsgaard and Egon Frandsen for their valued assistance in the field, and Anni Glud for constructing the microsensors used in this study. Jean-Pierre Gattuso and Bernard Gentili kindly provided the seabed light data that we used for the Arctic Ocean extrapolations. This study was supported by grants from the Commission for Scientific Research in Greenland (KVUG; GCRC6507), the UK Natural Environmental Research Council (NERC, NE/F018612/1, NE/F0122991/1, NE/G006415/1, NE/H525303/1), the European Research Council through an Advanced Grant (ERC-2010-AdG20100224), the Danish National Research Foundation (DNRF53), the Carlsberg Foundation (2013_01_0532), the Danish Environmental Protection Agency (DANCEA), and the Arctic Research Centre (ARC, Aarhus University). This work is a contribution to the Greenland Ecosystem Monitoring program (www.G-E-M.dk).

LITERATURE CITED

Aller RC (2014) Sedimentary diagenesis, depositional environments, and benthic fluxes. In: Holland HD, Turekian KK (eds) Treatise on geochemistry, Vol 8. Elsevier, Oxford, p 293–334

Arrigo KR, van Dijken GL (2011) Secular trends in Arctic ocean net primary production. J Geophys Res C Oceans 116:C09011, doi:10.1029/2011JC007151

Attard KM, Glud RN, McGinnis DF, Rysgaard S (2014) Seasonal rates of benthic primary production in a Greenland fjord measured by aquatic eddy correlation. Limnol Oceanogr 59:1555–1569

Attard KM, Stahl H, Kamenos NA, Turner G, Burdett HL, Glud RN (2015) Benthic oxygen exchange in a live coralline algal bed and an adjacent sandy habitat: an eddy covariance study. Mar Ecol Prog Ser 535:99–115

Babin M, Bélanger S, Ellingsen I, Forest A and others (2015) Estimation of primary production in the Arctic Ocean using ocean colour remote sensing and coupled physical–biological models: strengths, limitations and how they compare. Prog Oceanogr 139:197–220

Baldocchi DD (2003) Assessing the eddy covariance technique for evaluating carbon dioxide exchange rates of ecosystems: past, present and future. Glob Change Biol 9:479–492

Barber DG, Hop H, Mundy CJ, Else B and others (2015) Selected physical, biological and biogeochemical implications of a rapidly changing arctic marginal ice zone. Prog Oceanogr 139:122–150

Barnhart KR, Overeem I, Anderson RS (2014) The effect of changing sea ice on the physical vulnerability of arctic coasts. Cryosphere 8:1777–1799

Berg P, Huettel M (2008) Monitoring the seafloor using the noninvasive eddy correlation technique: integrated benthic exchange dynamics. Oceanography (Wash DC) 21: 164–167

Berg P, Risgaard-Petersen N, Rysgaard S (1998) Interpretation of measured concentration profiles in sediment pore water. Limnol Oceanogr 43:1500–1510

Berg P, Roy H, Janssen F, Meyer V, Jørgensen BB, Huettel M, de Beer D (2003) Oxygen uptake by aquatic sediments measured with a novel non-invasive eddy-correlation technique. Mar Ecol Prog Ser 261:75–83

Berg P, Roy H, Wiberg PL (2007) Eddy correlation flux measurements: the sediment surface area that contributes to the flux. Limnol Oceanogr 52:1672–1684

Berg P, Long MH, Huettel M, Rheuban JE and others (2013) Eddy correlation measurements of oxygen fluxes in permeable sediments exposed to varying current flow and light. Limnol Oceanogr 58:1329–1343

Blicher ME, Sejr MK (2011) Abundance, oxygen consumption and carbon demand of brittle stars in Young Sound and the NE Greenland shelf. Mar Ecol Prog Ser 422: 139–144

Blicher ME, Sejr MK, Rysgaard S (2009) High carbon demand of dominant macrozoobenthic species indicates their central role in ecosystem carbon flow in a sub-Arctic fjord. Mar Ecol Prog Ser 383:127–140

Borum J, Pedersen MF, Krause-Jensen D, Christensen PB, Nielsen K (2002) Biomass, photosynthesis and growth of *Laminaria saccharina* in a high-arctic fjord, NE Greenland. Mar Biol 141:11–19

Cahoon LB (1999) The role of benthic microalgae in neritic ecosystems. Oceanogr Mar Biol Annu Rev 37:47–86

Christensen B, Vedel A, Kristensen E (2000) Carbon and nitrogen fluxes in sediment inhabited by suspension-feeding (*Nereis diversicolor*) and non-suspension-feeding (*N. virens*) polychaetes. Mar Ecol Prog Ser 192:203–217

Conlan KE, Kvitek RG (2005) Recolonization of soft-sediment ice scours on an exposed Arctic coast. Mar Ecol Prog Ser 286:21–42

Dalsgaard T (2003) Benthic primary production and nutrient cycling in sediments with benthic microalgae and transient accumulation of macroalgae. Limnol Oceanogr 48: 2138–2150

Donis D, Holtappels M, Noss C, Cathalot C and others (2015) An assessment of the precision and confidence of aquatic eddy correlation measurements. J Atmos Ocean Technol 32:642–655

Duarte CM, Middelburg JJ, Caraco N (2005) Major role of marine vegetation on the oceanic carbon cycle. Biogeosciences 2:1–8

Fenchel T, Glud RN (2000) Benthic primary production and O_2–CO_2 dynamics in a shallow-water sediment: spatial and temporal heterogeneity. Ophelia 53:159–171

Gattuso JP, Gentili B, Duarte CM, Kleypas JA, Middelburg JJ, Antoine D (2006) Light availability in the coastal ocean: impact on the distribution of benthic photosynthetic organisms and their contribution to primary production. Biogeosciences 3:489–513

Glud RN (2008) Oxygen dynamics of marine sediments. Mar Biol Res 4:243–289

Glud RN, Blackburn N (2002) The effects of chamber size on benthic oxygen uptake measurements: a simulation study. Ophelia 56:23–31

Glud RN, Rysgaard S (2007) The annual organic carbon budget of Young Sound, NE Greenland. In: Rysgaard S, Glud RN (eds) Carbon cycling in Arctic marine ecosystems: case study Young Sound. Meddr Grønland Biosci 58:190–203

Glud RN, Holby O, Hoffmann F, Canfield DE (1998) Benthic mineralization and exchange in Arctic sediments (Svalbard, Norway). Mar Ecol Prog Ser 173:237–251

Glud RN, Risgaard-Petersen N, Thamdrup B, Fossing H, Rysgaard S (2000) Benthic carbon mineralization in a high-Arctic sound (Young Sound, NE Greenland). Mar Ecol Prog Ser 206:59–71

Glud RN, Kuhl M, Wenzhofer F, Rysgaard S (2002) Benthic diatoms of a high Arctic fjord (Young Sound, NE Greenland): importance for ecosystem primary production. Mar Ecol Prog Ser 238:15–29

Glud RN, Gundersen JK, Roy H, Jorgensen BB (2003) Seasonal dynamics of benthic O_2 uptake in a semienclosed bay: importance of diffusion and faunal activity. Limnol Oceanogr 48:1265–1276

Glud RN, Rysgaard S, Kuhl M, Hansen JW (2007) The sea ice in Young Sound: implications for carbon cycling. In: Rysgaard S, Glud RN (eds) Carbon cycling in Arctic marine ecosystems: case study Young Sound. Meddr Grønland Biosci 58:62–85

Glud RN, Woelfel J, Karsten U, Kuhl M, Rysgaard S (2009) Benthic microalgal production in the arctic: applied methods and status of the current database. Bot Mar 52: 559–571

Glud RN, Berg P, Hume A, Batty P, Blicher ME, Lennert K, Rysgaard S (2010) Benthic O_2 exchange across hard-bottom substrates quantified by eddy correlation in a sub-Arctic fjord. Mar Ecol Prog Ser 417:1–12

Grebmeier JM, Bluhm BA, Cooper LW, Danielson SL and others (2015) Ecosystem characteristics and processes facilitating persistent macrobenthic biomass hotspots and associated benthivory in the Pacific Arctic. Prog Oceanogr 136:92–114

Gundersen JK, Ramsing NB, Glud RN (1998) Predicting the signal of O_2 microsensors from physical dimensions, temperature, salinity, and O_2 concentration. Limnol Oceanogr 43:1932–1937

Gutt J (2001) On the direct impact of ice on marine benthic communities, a review. Polar Biol 24:553–564

Hancke K, Glud RN (2004) Temperature effects on respiration and photosynthesis in three diatom-dominated benthic communities. Aquat Microb Ecol 37:265–281

Holtappels M, Glud RN, Donis D, Liu B, Hume A, Wenzhofer F, Kuypers MMM (2013) Effects of transient bottom water currents and oxygen concentrations on benthic exchange rates as assessed by eddy correlation measurements. J Geophys Res C Oceans 118:1157–1169

Holtappels M, Noss C, Hancke K, Cathalot C, McGinnis DF, Lorke A, Glud RN (2015) Aquatic eddy correlation: quantifying the artificial flux caused by stirring-sensitive O_2 sensors. PLoS ONE 10:e0116564

Hop H, Pearson T, Hegseth EN, Kovacs KM and others (2002) The marine ecosystem of Kongsfjorden, Svalbard. Polar Res 21:167–208

Hume AC, Berg P, McGlathery KJ (2011) Dissolved oxygen fluxes and ecosystem metabolism in an eelgrass (*Zostera marina*) meadow measured with the eddy correlation technique. Limnol Oceanogr 56:86–96

Iversen N, Jorgensen BB (1993) Diffusion-coefficients of sulfate and methane in marine-sediments: influence of porosity. Geochim Cosmochim Acta 57:571–578

Jakobsson M, Macnab R, Mayer L, Anderson R and others (2008) An improved bathymetric portrayal of the Arctic Ocean: implications for ocean modeling and geological, geophysical and oceanographic analyses. Geophys Res Lett 35:L07602, doi:10.1029/2008GL033520

Kostka JE, Thamdrup B, Glud RN, Canfield DE (1999) Rates and pathways of carbon oxidation in permanently cold arctic sediments. Mar Ecol Prog Ser 180:7–21

Krause-Jensen D, Kuhl M, Christensen PB, Borum J (2007) Benthic primary production in Young Sound, Northeast Greenland. In: Rysgaard S, Glud RN (eds) Carbon cycling in Arctic marine ecosystems: case study Young Sound. Meddr Grønland Bioscience 58:160–173

Kristensen E, Penha-Lopes G, Delefosse M, Valdemarsen T, Quintana CO, Banta GT (2012) What is bioturbation? The need for a precise definition for fauna in aquatic sciences. Mar Ecol Prog Ser 446:285–302

Kuhl M, Glud RN, Borum J, Roberts R, Rysgaard S (2001) Photosynthetic performance of surface-associated algae below sea ice as measured with a pulse amplitude-modulated (PAM) fluorometer and O_2 microsensors. Mar Ecol Prog Ser 223:1–14

Long MH, Berg P, de Beer D, Zieman JC (2013) *In situ* coral reef oxygen metabolism: an eddy correlation study. PLoS ONE 8:e58581

Lorke A, McGinnis DF, Maeck A (2013) Eddy-correlation measurements of benthic fluxes under complex flow conditions: effects of coordinate transformations and averaging time scales. Limnol Oceanogr Methods 11:425–437

Lorrai C, McGinnis DF, Berg P, Brand A, Wuest A (2010) Application of oxygen eddy correlation in aquatic systems. J Atmos Ocean Technol 27:1533–1546

MacIntyre HL, Geider RJ, Miller DC (1996) Microphytobenthos: the ecological role of the 'secret garden' of unvegetated, shallow-water marine habitats. 1. Distribution, abundance and primary production. Estuaries 19:186–201

McGinnis DF, Berg P, Brand A, Lorrai C, Edmonds TJ, Wuest A (2008) Measurements of eddy correlation oxygen fluxes in shallow freshwaters: towards routine applications and analysis. Geophys Res Lett 35:L04403, doi: 10.1029/2007GL032747

McGinnis DF, Cherednichenko S, Sommer S, Berg P and others (2011) Simple, robust eddy correlation amplifier for aquatic dissolved oxygen and hydrogen sulfide flux measurements. Limnol Oceanogr Methods 9:340–347

McGinnis DF, Sommer S, Lorke A, Glud RN, Linke P (2014) Quantifying tidally driven benthic oxygen exchange across permeable sediments: an aquatic eddy correlation study. J Geophys Res C Oceans 119:6918–6932

Middelburg JJ, Duarte CM, Gattuso JP (2005) Respiration in coastal benthic communities. In: del Giorgio P, Williams

P (eds) Respiration in aquatic systems. Oxford University Press, Oxford, p 206–224

Mori N, Suzuki T, Kakuno S (2007) Noise of acoustic doppler velocimeter data in bubbly flows. J Eng Mech 133:122–125

Piepenburg D, Blackburn TH, von Dorrien CF, Gutt J and others (1995) Partitioning of benthic community respiration in the Arctic (northwestern Barents sea). Mar Ecol Prog Ser 118:199–213

Platt T, Gallegos CL, Harrison WG (1980) Photoinhibition of photosynthesis in natural assemblages of marine-phytoplankton. J Mar Res 38:687–701

Quintana CO, Kristensen E, Valdemarsen T (2013) Impact of the invasive polychaete *Marenzelleria viridis* on the biogeochemistry of sandy marine sediments. Biogeochemistry 115:95–109

Rasmussen H, Jorgensen BB (1992) Microelectrode studies of seasonal oxygen uptake in a coastal sediment: role of molecular-diffusion. Mar Ecol Prog Ser 81:289–303

Revsbech NP (1989) An oxygen microsensor with a guard cathode. Limnol Oceanogr 34:474–478

Rheuban JE, Berg P (2013) The effects of spatial and temporal variability at the sediment surface on aquatic eddy correlation flux measurements. Limnol Oceanogr Methods 11:351–359

Roberts RD, Kuhl M, Glud RN, Rysgaard S (2002) Primary production of crustose coralline red algae in a high arctic fjord. J Phycol 38:273–283

Rovelli L, Attard KM, Bryant LD, Flogel S and others (2015) Benthic O_2 uptake of two cold-water coral communities estimated with the non-invasive eddy correlation technique. Mar Ecol Prog Ser 525:97–104

Rysgaard S, Glud RN (eds) (2007) Carbon cycling in Arctic marine ecosystems: case study Young Sound. Meddr Grønland Biosci 58, Copenhagen

Rysgaard S, Sejr MK (2007) Vertical flux of particulate organic matter in a high arctic fjord: relative importance of terrestrial and marine sources. In: Rysgaard S, Glud RN (eds) Carbon cycling in Arctic marine ecosystems: case study Young Sound. Meddr Grønland Biosci 58: 110–119

Rysgaard S, Finster K, Dahlgaard H (1996) Primary production, nutrient dynamics and mineralisation in a northeastern Greenland fjord during the summer thaw. Polar Biol 16:497–506

Rysgaard S, Nielsen TG, Hansen BW (1999) Seasonal variation in nutrients, pelagic primary production and grazing in a high-Arctic coastal marine ecosystem, Young Sound, Northeast Greenland. Mar Ecol Prog Ser 179:13–25

Rysgaard S, Vang T, Stjernholm M, Rasmussen B, Windelin A, Kiilsholm S (2003) Physical conditions, carbon transport, and climate change impacts in a northeast Greenland fjord. Arct Antarct Alp Res 35:301–312

Sejr MK, Christensen PB (2007) Growth, production, and carbon demand of macrofauna in Young Sound, with special emphasis on bivalves *Hiatella arctica* and *Mya truncata*. In: Rysgaard S, Glud RN (eds) Carbon cycling in Arctic marine ecosystems: case study Young Sound. Meddr Grønland Biosci 58:122–135

Sejr MK, Jensen KT, Rysgaard S (2000) Macrozoobenthic community structure in a high-Arctic east Greenland fjord. Polar Biol 23:792–801

Sejr MK, Petersen JK, Jensen KT, Rysgaard S (2004) Effects of food concentration on clearance rate and energy budget of the arctic bivalve *Hiatella arctica* (L) at subzero temperature. J Exp Mar Biol Ecol 311:171–183

Thamdrup B, Glud RN, Hansen JW (2007) Benthic carbon cycling in Young Sound, Northeast Greenland. In: Rysgaard S, Glud RN (eds) Carbon cycling in Arctic marine ecosystems: case study Young Sound. Meddr Grønland Biosci 58:138–157

Wenzhofer F, Glud RN (2004) Small-scale spatial and temporal variability in coastal benthic O_2 dynamics: effects of fauna activity. Limnol Oceanogr 49:1471–1481

Woelfel J, Schumann R, Peine F, Flohr A and others (2010) Microphytobenthos of Arctic Kongsfjorden (Svalbard, Norway): biomass and potential primary production along the shore line. Polar Biol 33:1239–1253

Zacher K, Rautenberger R, Hanelt D, Wulff A, Wiencke C (2009) The abiotic environment of polar marine benthic algae. Bot Mar 52:483–490

Editorial responsibility: Martin Solan, Southampton, UK

Submitted: December 14, 2015; Accepted: May 23, 2016
Proofs received from author(s): July 14, 2016